Study on Mechanical Mechanism of Kink Folds via BEM

Wen-Jeng Huang [1], **Yusheng Liang** [2]
[1]Graduate Institute of Applied Geology, National Central University
[2]Graduate Institute of Geophysics, National Central University
Huang22@ncu.edu.tw
NSC Project: NSC 101-2116-M-008-019

ABSTRACT

Kink folds are distinguished by sharp hinges, straight limbs, and an asymmetry expressed by a short limb connecting two longer limbs. The folds are not truly flexural slip folds, because the slip between layers is highly localized; that is, just within kink bands. We use boundary element methods to develop multilayer models consisting of interface-slip in an elastic medium with possibly different cohesion and friction on interfaces of adjacent layers. We show that the properties of interfaces (i.e., cohesion and friction) and initial differential stress play important roles in finite forms of folds. We find a multilayer with certain cohesion stand-alone on its interfaces can produce kink bands under compression parallel to the interface but with friction only cannot. We find that the lower bound of stand-alone cohesion divided by Young's modulus ranges from 10^{-3} to 10^{-2} and friction cannot produce kink bands if the ratio of the vertical initial remote stress to horizontal initial remote stress is small than 0.2 under the shortening of 36% with an incremental far-field strain of 0.02 for multilayer models of 16 interfaces.

Keywords: kink folds, kink bands, coulomb criterion, multilayer, folding, buckling.

1. INTRODUCTION

Kink folds are distinguished by sharp hinges, straight limbs, and an asymmetry expressed by a short limb connecting two longer limbs [1]. The folds are not truly flexural slip folds, because the slip between layers is highly localized; that is, just within kink bands. The individual kink-bands range in size over at least five orders of magnitude from millimeter [2] to hectometer [3] and appear in numerous kinds of materials, such as organic crystals [4], card decks [5], rubber laminates [6], phyllites [7]. No matter what material kink bands may form within, its structure is always layered or fabric in terms of scale. Namely, they are anisotropic in mechanical sense. A few experimental works [e.g., 7] have solved much of mystery of kink bands. Theoretical works [e.g., 8; 9; 10; 11] gave insight into how the kink folds may form. The goal of the study is to apply the coulomb criterion to the interlayer properties and resolve the conditions in which the kink folds appear.

2. Theories of multilayer buckling

The concept of amplification factor is relevant in a general way to multilayer buckling. The theory of folding of initial perturbations in isolated layers or multilayers is quite mature [e.g., 12; 13; 14; 15; 16; 17; 18]. Of particular relevance to this paper are theoretical studies of the physical conditions of multilayer folding that lead to significant amplification of initially small perturbations. In linear, homogenous materials, the rate at which an initial perturbation is amplified is a function of the number of layers in the multilayer, *N*, the thickness of individual layers, *h*, and the wavelength, *L*, of the initial perturbation. The rate at which initial sinusoidal perturbations are amplified by buckling under horizontal compression was quantified by Biot [19] and Fletcher [15] as the "amplification factor". The amplification factor is a scalar quantity that determines the rate at which the amplitude of an initially small perturbation grows with increased shortening of the medium [e.g., 17]

Fig. 1 produced from the folding theory developed by Johnson and Pfaff [21] shows the amplification factor as a function of the wavelength of the perturbation normalized by the thickness of a single layer. The layers have viscosity equal to the surrounding media and free slip at layer contacts. The amplification factor is shown for multilayers with two, four, or ten layers. Fig. 1 illustrates that the amplification factor (i.e., the rate at which the amplitude grows) increases with the number of layers in the multilayer. Also, for a given layer thickness and number of layers, there is a so-called dominant wavelength at which the amplification factor is largest and the fold grows the fastest (the peak of the curves). Thus, Fig. 1 demonstrates the rather intuitive result that very broad or very narrow initial perturbations, relative to the thickness of the layers, grow in amplitude more slowly than perturbations with a dominant wavelength, and perturbations in a multilayer with many thin layers grow in amplitude more quickly than in a multilayer of the same total thickness but composed of a few thick layers. Considering the purpose of the research, the initial perturbations and the ratio of thickness of single layer to wavelength are fixed for all the models. The initial perturbation is a sinusoidal shape with a ratio, 0.0006, of amplitude to wavelength. The ratio, 0.02, of thickness of single layer to wavelength is arbitrarily picked.

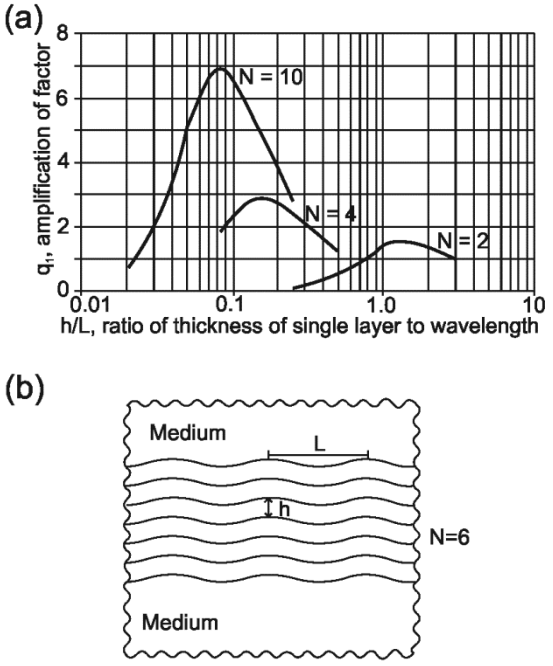

Figure 1 (a) Plots of amplification factor for periodic folds in viscous layers as a function of wavelength, *L*, normalized by the thickness of a single layer, *h*. *N* indicates number of layers in multilayer. Layers slip freely at contacts. Layers and surrounding medium have same viscosity. The plots are produce by using the folding theory developed by Johnson and Pfaff [20]. (b) Illustration of a multilayer bounded above and below by semi-infinite media. The number of layers in the multilayer, *N*, is 6.

3. BOUNDARY ELEMENT MODEL OF MULTIPLE-LAYER FOLDING

We develop a boundary element model to investigate the formation of kink folds by buckling. The boundary element method (BEM) is different from the finite element method (FEM) in that the medium is discretized only at boundaries in the BEM whereas the entire medium is discretized in the FEM.

3.1. Basic Formulation

In layered sedimentary or foliated metamorphic rocks, mechanical interfaces between sedimentary and foliated layers may form because of differences in physical properties at the interfaces such as grain size and cementation. Soft layers interbedded with stiff layers may localize shear, allowing the stiff layers to slide past each other. These conditions are important in folding because the bedding-plane slip can allow the strata to mechanically buckle with flexural slip. We model these conditions with multiple elastic layers with frictional contacts (Fig. 2).

The basic geometry and boundary conditions of models are illustrated in Fig. 2. We model mechanical layers with initially horizontal slip surfaces of finite length within an otherwise homogeneous elastic half-space. In general, the layers are assumed to slip according to a Coulomb friction law, $|\tau_s| \le C + \mu\sigma_n$, where τ_s is shear stress, C is cohesion, μ is the coefficient of friction, and σ_n is normal stress (compression is positive). The entire medium is subjected to increments of either uniform strain. If the shear stress on layers exceeds the strength as defined by the Coulomb friction law during each increment of far-field strain the interfaces slip in order to reduce the shear stress to the strength.

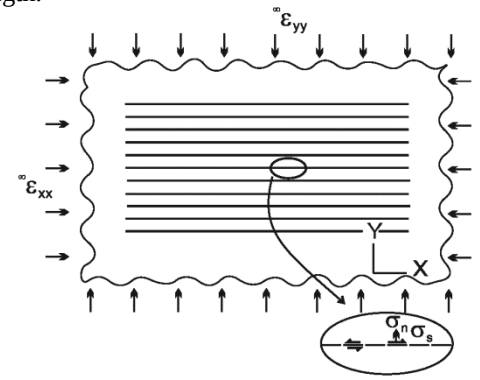

Figure 2 Geometry and boundary conditions of multilayer model in an elastic medium with mechanical layering. Notation is σ: stress, σ_n: normal traction, σ_s: shear traction, and ${}^{ff}\varepsilon$: remote strain. Wiggly edges indicate that the medium extends to infinity.

The numerical technique of the boundary element method has been clearly described by Crouch and Starfield [21]. Our boundary element algorithm is largely similar to their two-dimensional displacement discontinuity method (TWODD) which was succinctly summarized by Martel and Muller [22]. We formulate the elastic boundary element models using the solution for an edge dislocation in an isotropic, homogeneous, elastic half-space assuming infinitely long faults and bedding contacts in the strike direction (2D plane-strain conditions).

We give a brief outline of our formulation of the boundary element model. Assume we have a $N \times 1$ vector of incremental values of the dip component of slip, *s*, on *N* patches. From the solution for a 2D edge dislocation, we can relate the vector of shear stresses, σ_s, and normal stresses, σ_n, at the center of each patch to slip on all the patches through the $N \times N$ matrixes, $G_{\sigma s}$, and $G_{\sigma n}$, respectively,

$$\sigma_s = G_{\sigma s} s \ ;$$
$$\sigma_n = G_{\sigma n} s \, . \qquad (1)$$

We assume a coordinate system with *x* in the horizontal direction and *y* in the vertical direction. We apply increments of far-field uniform strain,

$${}^{ff}\varepsilon_{xx} = \text{constant},$$
$${}^{ff}\varepsilon_{yy} = -{}^{ff}\varepsilon_{xx}\nu/(1-\nu),$$
$${}^{ff}\varepsilon_{xy} = 0, \qquad (2)$$

with corresponding uniform far-field stress,

$${}^{ff}\sigma_{yy} = {}^{ff}\sigma_{xy} = 0,$$

$$^{ff}\sigma_{xx} = 2\mu\,^{ff}\varepsilon_{xx} + \lambda\left(^{ff}\varepsilon_{xx} + {}^{ff}\varepsilon_{yy}\right), \qquad (3)$$

where λ and μ are Lame's elastic constants, $\lambda = 2\mu\nu/(1-2\nu)$, and ν is Poisson's ratio. We normalize all stresses by μ and assume ν = 0.25. From the far-field stress we compute the shear component of stress resolved onto each patch, $^{ff}\sigma_s$. We satisfy the condition that the shear stress is smaller than or equal to $C + \mu\sigma_n$ on each patch after each increment of deformation,

$$^{ff}\sigma_s + G_\sigma s \le C + \mu\sigma_n . \qquad (4)$$

The distribution of incremental slip, *s*, on the patches is attained based on this condition

$N \times N$ matrices $_xG_d$ and $_yG_d$ relating the *x* and *y* components of displacements of the endpoints of the patches to the slip on each patch is constructed using the solution for the edge dislocation. Note that we only specify one boundary condition and solve for only one slip component on each patch because we assume that the normal component of displacement discontinuity across patches is zero. Then the incremental displacements, Δu_x and Δu_y, of the patch endpoints during the small increment of deformation are calculated as

$$\Delta u_x = {}_x G_d s + {}^{ff}\Delta u_x ,$$
$$\Delta u_y = {}_y G_d s + {}^{ff}\Delta u_y , \qquad (5)$$

with the contribution to the displacements from the far-field strain being

$$^{ff}\Delta u_x = x\,^{ff}\varepsilon_{xx},$$
$$^{ff}\Delta u_y = y\,^{ff}\varepsilon_{yy}, \qquad (6)$$

Positions of new patch endpoints are calculated from the previous endpoints and the incremental displacements, and then a new increment of far-field strain is applied and the calculations in equations (1)-(6) are repeated.

It is important to recognize that we have adopted the linear (infinitesimal strain) elastic solution for an edge dislocation, yet we do not restrict our analysis to small strains. We assume that each increment of deformation can be modeled with the small strain theory, ignoring nonlinear effects due to the initial stress condition at the beginning of each increment. This is equivalent to assuming that the elastic stresses in the medium surrounding the faults and layer interfaces are somehow relaxed before the beginning of the next deformation increment. Inelastic processes for relaxing stresses include: micro-cracking [e.g. 23], grain boundary sliding [e.g. 24], twinning [e.g. 25], pressure solution [e.g. 26], recrystallization, and so on [e.g. 27]. Because we do not account for these processes in our model, results from this analysis must be viewed with mindfulness of the assumptions. Furthermore, we assume an incremental far-field strain of $^{ff}\varepsilon_{xx}$ = -0.02 in all the applications in this paper which is about an order of magnitude larger strain than permissible by linear elasticity theory. However, we examine the effect of the incremental far-field strain with a range of magnitudes between 0.005 and 0.2 on the final fold form. We find that the increments of deformation equal to or smaller than 0.02 do not produce an appreciable difference in the final fold form indicating that our choice of incremental far-field strain is not a severe limitation. Fig. 3 shows the amplification increases with the amount of interfaces under the shortening of 35.9% and others. From rock experiments [7], rock samples are commonly smashed under the shortening of larger than 40%. Therefore, for simplicity and efficiency, we adopt 16 interfaces and applied shortening of for all the models hereafter.

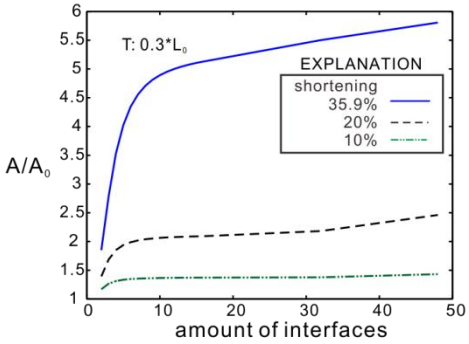

Figure 3 Growth of fold amplitude vs. number of interfaces under different shortenings

3.2. Effects of Parameters

There are three main parameters: friction angle and cohesion of interlayer property, and initial remote vertical stress in our models. The effects of these parameters are examined as follows. The models in Fig. 4 are frictional ($\mu \neq 0$) but cohesionless (C = 0) for the interfaces without remote vertical stress, i.e. $^{ff}\sigma_{yy}$ = 0. It shows frictional resistance has the potential to from kink folds. The models in Fig. 5 are cohesive ($C \neq 0$), but frictionless (μ = 0) for the interfaces without remote vertical stress. It shows cohesion alone can produce kink folds. The $^{ff}\sigma_{yy}$ alone for frictionless and cohesionless layers has no effect on the fold form. However, a combined effect of μ and $^{ff}\sigma_{yy}$ is seemingly able to from kink folds shown in Fig. 6.

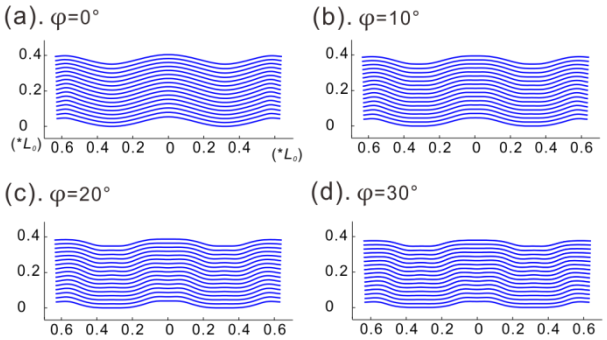

Figure 4 Model results for different frictions, μ, (i.e. $\tan\varphi$) but cohesionless (C = 0) for the interfaces without remote vertical stress, i.e. $^{ff}\sigma_{yy}$ = 0.

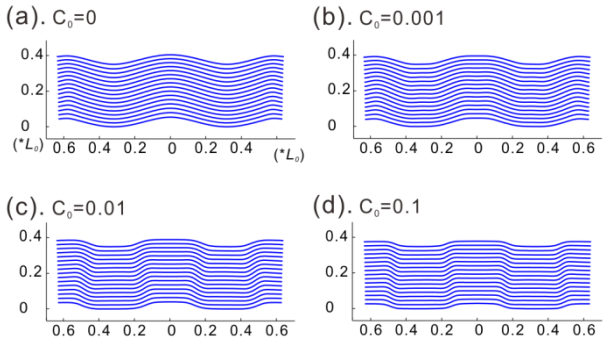

Figure 5 Model results for different cohesions but frictionless ($\mu = 0$) for the interfaces

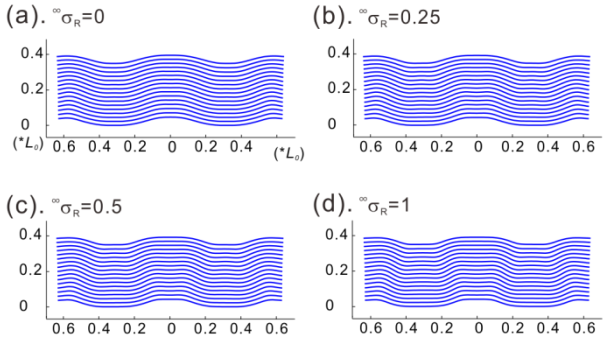

Figure 6 Model results for different normalized initial remote vertical stress, ${}^{\infty}\sigma_R$ (equal to ${}^{ff}\sigma_{yy}$ / ${}^{ff}\sigma_{xx}$) with a friction angle, φ , of 10 ° but cohesionless ($C = 0$) for the interfaces

4. SIMULATION RESULTS

Broad ranges of values for the three main parameters are examined on exploring the conditions under which kink folds may from. Two different loadings in view of its direction to the orientation of initial interfaces are presented. When the direction of shortening is parallel to the trend of initial interfaces, symmetric box kink-folds may form. When the direction of shortening is inclined to the trend of initial interfaces with a small angle, asymmetric shear kink-bands may form.

4.1. Symmetric box folds

With no surprise, symmetric folds results from certain amount of shortening parallel to the orientation of initial interfaces, for example, in Fig 7. Figs. 7b and 7d show that the distribution of slip along the interface is localized within the kink bands while the kink folds form. Fig. 8 shows that the fold forms change from sinusoidal to step-like with the increase of either μ (i.e. $\tan\varphi$) or ${}^{ff}\sigma_{yy}$ and both. The fig also indicates that a certain value of ${}^{ff}\sigma_{yy}$ is needed to form a perfect kink fold; however, the need of friction can be lowed while the ${}^{ff}\sigma_{yy}$ is relatively larger. The dashed lines in Figs 8 and 9 are artificial boundaries for different folds. Fig. 9 shows that the combined effect of C and μ results in a variety of fold forms and the region of kink folds expends with the increase of the ${}^{ff}\sigma_{yy}$.

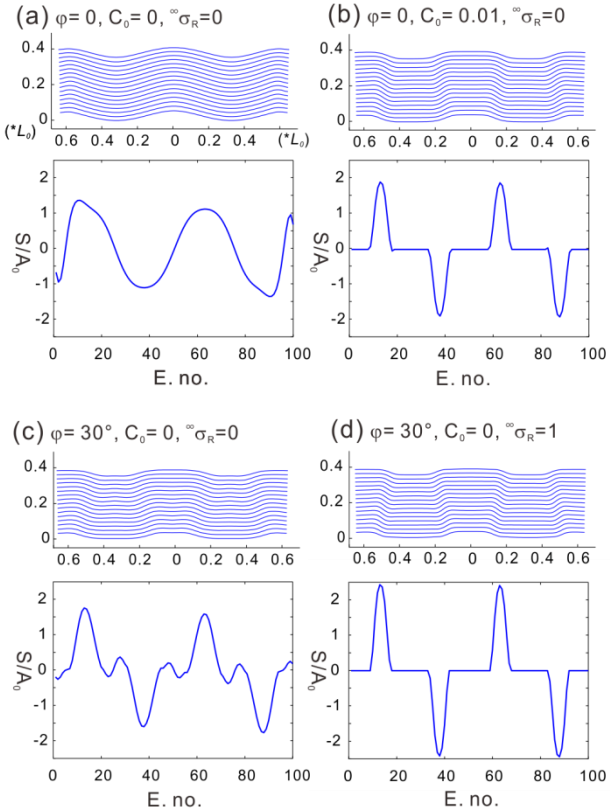

Figure 7 Model results and slip distributions along interface under different conditions. S, A_0, L_0 ,and E. no. denote slip, initial fold amplitude and wavelength, and element number, respectively.

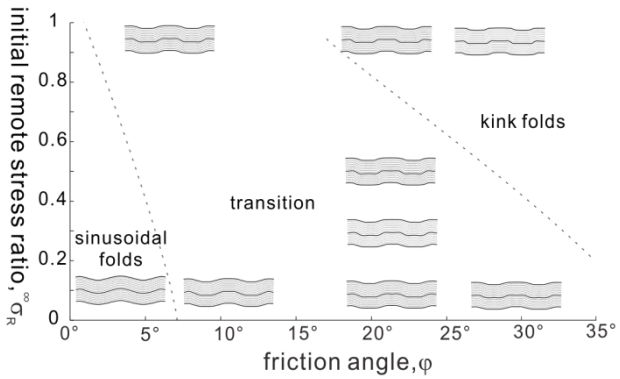

Figure 8 Sequential modeled folds under normalized initial remote vertical stress, ${}^{\infty}\sigma_R$, and friction angle, φ

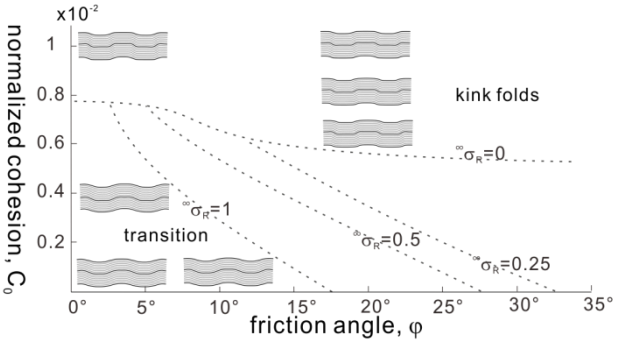

Figure 9 Sequential modeled folds under normalized cohesion, C_0 (that is, cohesion divided by Young's modulus), and friction angle, φ. The dashed lines are boundaries for different fold forms and labeled with a specified value of ${}^{\infty}\sigma_R$.

4.2. Asymmetric shear bands

Asymmetric shear kink-bands appear more commonly than symmetric box kink-folds in nature. Previous studies have indicated that asymmetric kink-bands can result from the shortening inclined to trend of initial interface [e.g., 7]. The direction of shortening for all the models presented in this section is inclined to the trend of initial interfaces with an angle of one degree. Fig. 10 shows how S-type sine-like folds gradually change to z-type kink bands with the increase of cohesion and their final distributions of slip along the interface. Fig shows larger μ and ${}^{ff}\sigma_{yy}$ can result in kink bands and may result in complex folds as well.

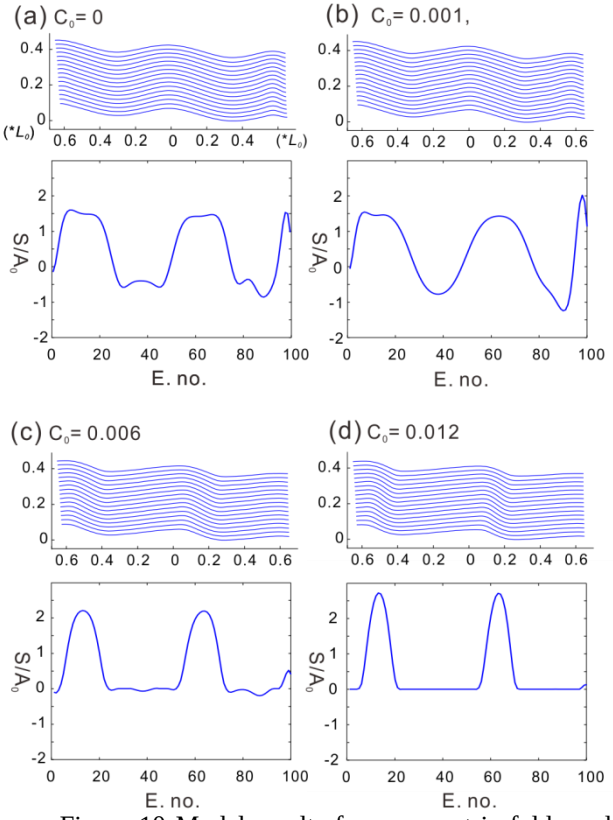

Figure 10 Model results for asymmetric folds and slip distributions along interface under different cohesions. The direction of shortening and the initial trend of interfaces intersect at an angle of 1 degree. S, A_0, L_0 ,and E. no. denote slip, initial fold amplitude and wavelength, and element number, respectively.

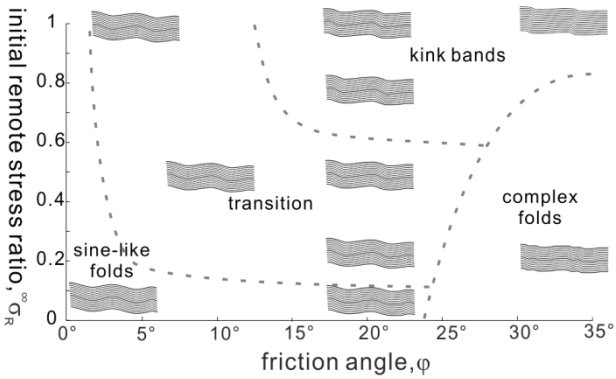

Figure 11 Sequential modeled asymmetric folds under normalized initial remote vertical stress, ${}^{\infty}\sigma_R$, and friction angle, φ. The direction of shortening and the initial trend of interfaces intersect at an angle of 1 degree.

5. DISCUSSION and CONCLUSIONS

The range of friction is largely between 0.6 and 0.85 for different rocks [28]. Namely, the frictional angle ranges from 30° to 40°. The magnitude of cohesion for many different rocks and ores is 1 to 10×10^7 Pa [29]. The magnitude of Young's modulus for different rocks is roughly 10^{10} Pa [30]. Those values mostly refer to the intact rocks or, say, non-layered rocks. Therefore, for layered rocks, such as laminated shales or phyllites, the values for their interface properties shall be lower but not possibly higher. Thus, our analyses shall cover all possible ranges that the kink bands may form in rocks if our models are valid.

In conclusion, the properties of interfaces (i.e., cohesion and friction) and initial differential stress play important roles in finite forms of folds. Multilayers with certain cohesion stand-alone on their interfaces can produce kink bands under compression parallel to the interface but with friction only cannot. The lower limit of the cohesion divided by Young's modulus is 10^{-3} to 10^{-2}. The ratio of the vertical remote stress to horizontal remote stress shall be larger than 0.2; otherwise, friction alone cannot produce kink bands.

ACKNOWLEDGEMENT

This research was supported by the National Science Council in Taiwan through Grant NSC 101-2116-M-008-019.

REFERENCES

[1] G.H. Davis, S. J. Reynolds and C.F. Kluth, *Structrual Geology of Rocks and Regions*, third edition, John Wiley & Sons, INC; 2012.
[2] E. Orowan, "A Type of Plastic Deformation New in Metals", *Nature*, No. 3788, June 6, 1942.
[3] D. P. Ashwin, "The structure and sedimentation of the Culm sediments between Boscastle and Bidford, N. Deveon." Unpublished Ph.D. Thesis, University of London.
[4] Mugge, *Neues Jahrb. f. Miner.* Vol. 1, 71, 1898.
[5] N.C. Gay and L.E. Weiss, "The Relationship between

Principal Stress Directions and the Geometry of Kinks in Foliated Rocks," *Tectonophysics*, Vol.21, 287, 1974

[6] R.E. Robertson, *J. Polymer Sci.*, Part A-2 7, 1315-1328, 1969.

[7] M.S. Paterson and L.E. Weiss, " Experimental Deformation and Folding in Phyllite", Geol. Soc. Am. Bull., Vol. 77, 343-374, 1966.

[8] J.P. Latham, "The Influence of Mechanical Anisotropy on the Development of Geological Structures," unpublished Ph.D. Thesis , University of London.

[9] J.G. Summer, " An Experimental and Theoretical Investigation of Multilayer Fold Development," Unpublished Ph.D. Thesis, University of London.

[10] P.R. Cobbold, "Mechanical effects of anisotropy during large finite deformations, " *Bull. de la Societe Geologique de la France*, Vol. 18, 1497-1510.

[11] A.M. Johnson and E. Honea, "A Theory of Concentric, Kink and Sinusoidal Folding and of Monoclonal Flexuring of Compressible, Elastic Multilayer. III. Transition from Sinusoidal to Concentric-like to Chevron Folds," *Tectonohysics*, Vol. 27, 1-38, 1975.

[12] M. A. Biot, "Exact Theory of Buckling of a Thick Slab," *Applied Scientific Research*, Section A, Vol. 12, 183-197, 1964.

[13] M.A. Biot, "Theory of Internal Buckling of a Confined Multilayered Structure," *Geol. Soc. Am. Bull.*, Vol. 76, 563-568, 1964

[14] W. M. Chappel, "Fold Shape and Rheology: the Folding of an Isolated Viscous-plastic Layer," *Tectonophysics*, Vol. 7, 97-116, 1969.

[15] R.C. Fletcher, "Folding of a Single Viscous Layer: Exact Infinitesimal-amplitude Solution," *Tectonophysics*, Vol. 39, 593-606, 1977.

[16] A.M. Johnson, *Styles of Folding*. Elsever Publishing Company, New York; 1977.

[17] A.M. Johnson and R. Fletcher, *Folding of Viscous Layers*, Columbia Univ. Press.; 1994.

[18] N.S. Mancktelow, "Finite-element Modeling of Single-layer Folding in Elasto-viscous Material: the Effect of Initial Perturbation Geometry," *Journal of Structural Geology*, Vol. 21, 161-177, 1999.

[19] M.A. Biot, "Theory of Folding of Stratified Viscoelastic Media and its Implications in Tectonics and Orogenesis," Geological Society of America Bulletin, Vol. 72, 1595-1620, 1961.

[20] A.M Johnson and V.J. Pfaff, "Parallel, Similar and Constrained Folds," *Engineering Geology*, Vol. 27, 115-180, 1989.

[21] S.L. Crouch and A. M. Starfield, *Boundary Element Methods in Solid Mechanics*, George Allen & Unwin Pulishers, London; 1983.

[22] S.J. Martel and J. Muller, "A Two-dimensional Boundary Element Method for Calculating Elastic Gravitational Stresses in Slopes," *Pure and Applied Geophysics*, Vol. 157, 989-1007, 2000.

[23] I.L. Meglis, R.E. Gagnon and R. P. Young, "Microcracking during Stress-relief of Polycrystalline Ice Formed at High Pressure," *Geophysical Research Letters*, Vol. 22(16), 2207-2210, 1995.

[24] T.G. Langdon, "Grain Boundary Sliding as a Deformation Mechanism During Creep," *Philosophical Magazine*, Vol. 22, 689-700, 1970.

[25] T. Yamashita and K. Ojima, "Deformation Twin Tips with Flat Surfaces in Pure Iron Crystals," *Journal of Election Microscopy*, Vol. 17(4), 301-308, 1968.

[26] K.R. McClay, " Pressure Solution and Coble Creep in Rocks and Minerals: a Review," *Journal of the Geological Society of London*, Vol. 134, 57-70, 1977.

[27] R.H. Sibson, "Earthquakes and Rock Deformation in Crustal Fault Zones," *Annual Review of Earth and Planetary Science*, Vol. 14, 25-50, 1986.

[28] J. Byerlee, "Friction of Rocks," *Pure and applied Geophysics*, Vol. 116(4), 615-626, 1978

[29] N. Lundborg, "Triaxial Shear of Some Swedish Rocks and Ores," Proc. 1st Cong. Int. Soc. Rock Mech., Lisbon, Vol. 1, 251-255, 1966.

[30] A.M. Johnson, *Physical Processes in Geology*, Freeman, Cooper &Company; 1970.